

Preparation and Elastic Properties of Helical Nanotubes Obtained by Atomic Layer Deposition with Carbon Nanocoils as Templates**

Yong Qin,* Yunseok Kim,* Lianbing Zhang, Seung-Mo Lee, Ren Bin Yang, AnLian Pan, Klaus Mathwig, Marin Alexe, Ulrich Gösele, and Mato Knez

Helical nanofibers and nanotubes of inorganic materials have application potential in various fields, such as catalysis, sensors, and functional and smart systems. Currently available helical nanomaterials include coiled carbon nanotubes,^[1] carbon nanocoils,^[2–4] silica nanosprings,^[5,6] silicon carbide nanosprings,^[7] and helical transition-metal (Ti, Ta, V) oxide nanotubes.^[8,9] The synthesis methods for helical nanomaterials rely mainly on catalytic chemical vapor deposition (CVD) and template approaches. The template method is usually applied to the synthesis of helical oxide nanotubes because it is relatively difficult to fabricate such tubular structures directly by CVD or physical vapor deposition (PVD).^[5,10,11] Carbon nanocoils are the most successfully synthesized by CVD with good reproducibility and high yields. Previously, helical metal and oxide nano- and microstructures have been synthesized by electrodeposition, electroless deposition, and sol-gel methods with carbon nanocoils or microcoils as templates.^[12–14] However, these coating methods do not provide convenient and simple control over the thickness and uniformity of the coatings because the templates have low chemical reactivity, small diameters, and particularly large surface curvature. Moreover, certain pretreatments and suitable surfactants are required to improve the wettability and chemical reactivity of the templates.

Atomic layer deposition (ALD) is a powerful growth technique for high-quality films. It utilizes the sequential exposure of reactants to substrates to achieve layer-by-layer film growth, which allows atomic-scale thickness control. Compared to traditional PVD or CVD methods, it shows outstanding advantages including precise thickness control,

large-scale uniformity, high conformality, and sharp interfaces. It is especially suitable for deposition of conformal films on substrates with complex geometries or porous structures. Straight Al₂O₃ and TiO₂ nanotubes have been prepared by ALD using carbon nanotubes, polymers, or viruses as templates.^[15–18]

Herein, we report the synthesis of various helical oxide nanotubes (Al₂O₃, SiO₂, TiO₂, HfO₂, and ZnAl₂O₄) by ALD using carbon nanocoils as templates. The helical morphology of the templates was well transcribed in the resulting nanotubes. Well-controlled thickness and excellent conformality were achieved. The mechanical properties of helical and straight Al₂O₃ nanotubes were measured by performing bending tests using atomic force microscopy (AFM). The helical nanotubes show much better elasticity than straight nanotubes due to their helical topography, which might be important for the use of such structures in devices relying on mechanical stability, for example, micro- or nanoelectromechanical systems.

Figure 1a shows a representative scanning electron microscopy (SEM) image of the starting carbon nanocoils used in this study. The carbon nanocoils have diameters of approximately 100 nm. They are tightly coiled and have very uniform coil pitches and coil diameters. By applying 50–200 ALD cycles for Al₂O₃ deposition, an amorphous Al₂O₃ film is coated on the nanocoils, which can be observed from the transmission electron microscopy (TEM) image shown in Figure 1b. The formed core/shell structures are clearly visible due to their different contrasts. The helical morphologies of the carbon nanocoils are well preserved, revealed by the uniform periodicity of coil pitches along the entire length. The outer surfaces of the shells are relatively smooth, like those of the initial templates. This indicates that the nanocoils can be coated by ALD with uniform coverage and perfect conformality, although they have a large surface curvature due to the small coil diameters and coil pitches.

The nanocoils were grown at a low temperature, and thus they are amorphous and contain a high content of hydrogen, thus leading to a low thermal stability as revealed by thermogravimetric analysis.^[19] The nanocoils can be completely removed by calcination even at a temperature as low as 350 °C in air. This redounds to their removal after ALD to obtain helical oxide nanotubes. Figure 1c–f shows Al₂O₃ nanotubes produced by 50, 100, 150, and 200 ALD cycles of Al₂O₃ deposition, respectively. It can be observed that these

[*] Dr. Y. Qin, Dr. Y. Kim, L. B. Zhang, S.-M. Lee, R. B. Yang, Dr. A. L. Pan, K. Mathwig, Dr. M. Alexe, Prof. U. Gösele,† Dr. M. Knez
Max Planck Institute of Microstructure Physics
Weinberg 2, 06120 Halle (Germany)
E-mail: yqin@mpi-halle.de; ykim@mpi-halle.de

[†] Deceased.

[**] This work was financially supported by the German Federal Ministry of Education and Research (BMBF) with the contract number FKZ 03X5507. Y.K. thanks the Alexander von Humboldt Foundation for a fellowship. We also acknowledge the focused ion beam work by Norbert Schammelt.

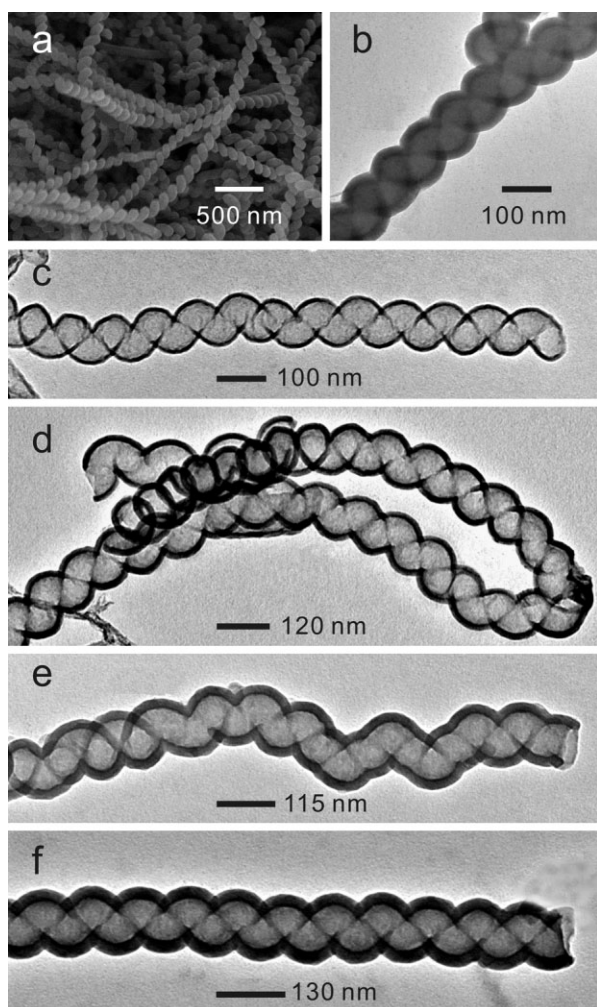


Figure 1. a) SEM image of carbon nanocoils. b) TEM image of Al_2O_3 -coated nanocoils obtained by applying 200 ALD cycles. c–f) TEM images of helical Al_2O_3 nanotubes obtained by applying 50, 100, 150, and 200 cycles of Al_2O_3 deposition, respectively. Scale bars for (b–f) indicate the outer diameters of these structures.

nanotubes show a helical morphology similar to that of the nanocoil templates. The center exhibits a brighter contrast than the shells, clearly revealing a tubular structure. No collapse of the shell materials occurred during the annealing process to remove the carbon cores. All nanotubes have a shell with a uniform thickness along the whole length of the nanotube. The shell thickness clearly increases with an increased number of ALD cycles. It amounts to about 5, 10, 15, and 20 nm, respectively, which corresponds to a growth rate of about 1 Å per cycle. Selected-area electron diffraction (SAED) reveals the amorphous nature of the Al_2O_3 shells. These results demonstrate that it is feasible to prepare helical oxide nanotubes with conveniently controlled wall thicknesses and good conformality by using carbon nanocoils as templates in ALD.

Helical SiO_2 , TiO_2 , and HfO_2 nanotubes were also synthesized by ALD using carbon nanocoils as templates. The SiO_2 nanotubes also preserve the helical morphology of the template (Figure 2a). The shell is about 25 nm thick for 400

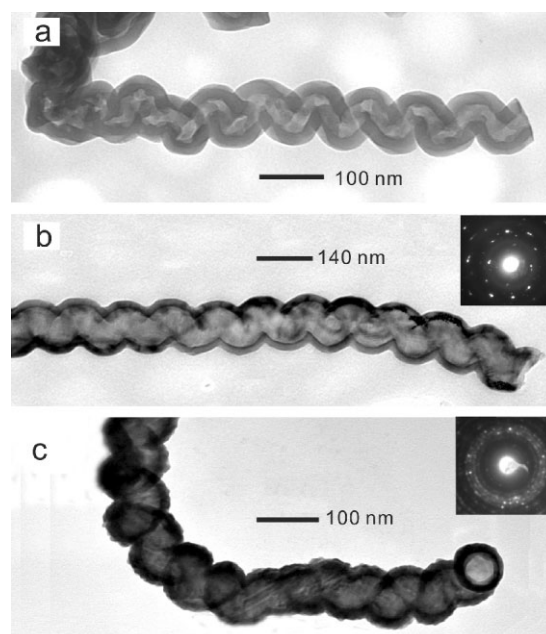


Figure 2. TEM images of helical nanotubes after removal of templates. a) SiO_2 , b) TiO_2 , and c) HfO_2 nanotubes. Insets show SAED patterns of these nanotubes.

ALD cycles with an amorphous structure revealed by SAED analysis. Figure 2b shows the obtained helical TiO_2 nanotubes with a shell thickness of 25 nm after 1000 ALD cycles. The outer surface of the nanotube is smoothly curved like the initial template and the coating is very conformal. SAED analysis (inset in Figure 2b) indicates that the shells have a polycrystalline anatase structure, which consists of high-quality nanocrystals within the helical tubular structure. The obtained helical HfO_2 nanotubes are displayed in Figure 2c. The shell thickness amounts to about 25 nm after 400 ALD cycles. The SAED pattern of the shell (inset in Figure 2c) indicates that it is also polycrystalline with a monoclinic structure. Due to the high atomic number of Hf, the shell produces a darker contrast that obscures the inner core.

The advantage of ALD enables us to prepare coaxial multilayer nanotubes. By changing precursors, desirable layers of multiple materials can be sequentially deposited. It is unnecessary to treat the samples during the deposition interval even if these materials differ much in their properties, such as electrical conductivity and wettability, which warrant great attention under other methods such as electrodeposition, sol-gel, etc. This allows us to conveniently fabricate helical tubular heterostructures with different functional outer and inner layers. Figure 3 displays helical coaxial nanotubes consisting of TiO_2 and Al_2O_3 layers after removal of the templates. The nanotube shown in Figure 3a was produced first by depositing 20 nm of TiO_2 and then 15 nm of Al_2O_3 . Because of the larger atomic number of Ti compared to that of Al, the TiO_2 layer shows a darker contrast resulting in clearly visible interfaces. A reverse sequence yields nanotubes with an inner Al_2O_3 layer and an outer TiO_2 layer as shown in Figure 3b. The interface is less clear because of the darker contrast of the outer layer of TiO_2 obscuring the inner Al_2O_3 layer, as indicated by the arrow.

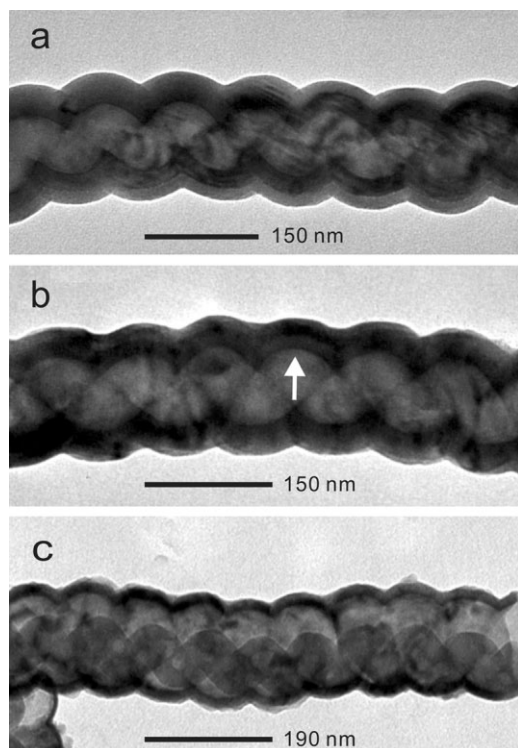


Figure 3. TEM images of helical multilayer nanotubes. a) $\text{Al}_2\text{O}_3/\text{TiO}_2$ nanotube obtained by coating first 20 nm of TiO_2 and then 15 nm of Al_2O_3 . b) $\text{TiO}_2/\text{Al}_2\text{O}_3$ nanotube obtained by reversing the coating sequence in (a). c) TiO_2 /carbon-nanocoil composite nanotube obtained by removing the Al_2O_3 layer (30 nm) between the nanocoil and the outer TiO_2 layer (20 nm) with a 10% H_3PO_4 aqueous solution at 45 °C for 6 h.

Regardless of the deposition sequence, both layers have a uniform thickness and the helical morphologies of the templates are well maintained. The deposited Al_2O_3 layer can also be used as a sacrificial material to create nanochannels with a complex structure for potential applications in nanofluidics. Figure 3c shows a TiO_2 /carbon-nanocoil composite nanotube, obtained by dissolving the 30-nm-thick Al_2O_3 layer sandwiched between the 20-nm-thick TiO_2 layer and the nanocoil templates (with a 10% H_3PO_4 aqueous solution). The carbon nanocoil sits on the inner wall of the TiO_2 nanotube and the void in between can be clearly observed.

This ALD-assisted template method is not limited to as-deposited single-phase or multilayer materials. Helical nanotubes of new materials can also be obtained through an interfacial solid-state reaction between the deposited multilayer materials. For example, helical ZnAl_2O_4 spinel nanotubes were fabricated by this approach. Figure 4a shows a TEM image of a carbon nanocoil coated first with 20 nm of Al_2O_3 and then 20 nm of ZnO . The helical surfaces are well preserved although the ZnO layer makes the interface of these different layers invisible. By annealing the sample at 700 °C for 3 h in air, a solid-state reaction was initiated by the diffusion of the outer ZnO material into the inner Al_2O_3 layer by the Kirkendall effect.^[20] At the same time, the carbon template was removed leading to a tubular structure. In terms of the stoichiometry, the amount of

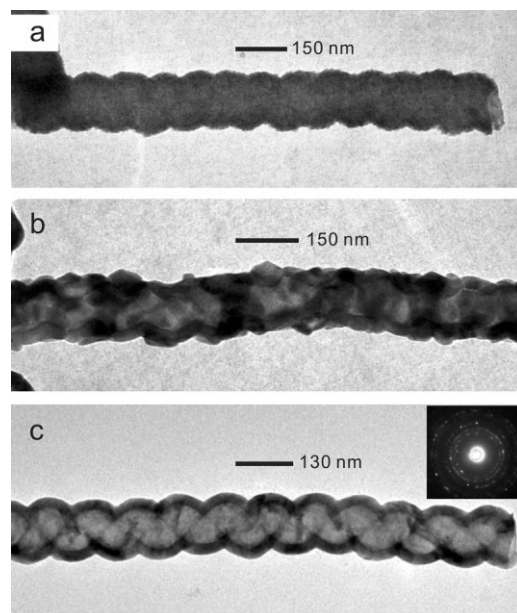


Figure 4. TEM images of a) a carbon nanocoil coated first by 20 nm of Al_2O_3 and then 20 nm of ZnO , b) a coated nanocoil after annealing at 700 °C for 3 h in air, and c) a helical spinel nanotube after removal of the excess ZnO with a HCl aqueous solution and its SAED pattern (inset).

ZnO is sufficient for the thorough transformation of the Al_2O_3 layer to a spinel. Figure 4b shows a coated nanocoil after annealing. The excess ZnO recrystallized to produce crystals with larger sizes during annealing, which are randomly distributed on the outer surface of the nanotube resulting in a rough surface. Figure 4c reveals the final helical spinel nanotube after the excess ZnO was removed in aqueous HCl . The thickness of the shell is uniform and identical with that of the original Al_2O_3 layer, thus confirming the occurrence of the Kirkendall effect. The SAED pattern (inset in Figure 4c) indicates that the shell is polycrystalline with a face-centered cubic structure.

The elastic properties of the produced helical nanotubes were measured with Al_2O_3 nanotubes as examples. For mechanical measurements, helical Al_2O_3 nanotubes were distributed on a Si substrate with square pits (inverted pyramids). Pt pads were deposited on both ends of the nanotubes using electron-induced deposition for fixation (Figure 5a–c).^[21] A commercial AFM instrument was used to conduct bending tests on the nanotubes. To obtain the elastic modulus of the nanotubes, force–deflection (F – D) curves were measured at the helical nanotubes. We pushed the nanotubes at their midpoint with calibrated Si cantilevers. The deflection of the cantilever was monitored during manipulation of the tip and the corresponding trace was recorded. $\tan \alpha$ and $\tan \beta$ were extracted from the slopes of these F – D curves. For comparison, a reference sample with a straight nanotube of similar dimensions was also prepared and measured (Figure 5d–f). We use the simple beam theory for a cantilever beam and assume that both helical and straight nanotubes have the second moment as a filled cylinder and that the beam has a uniform and

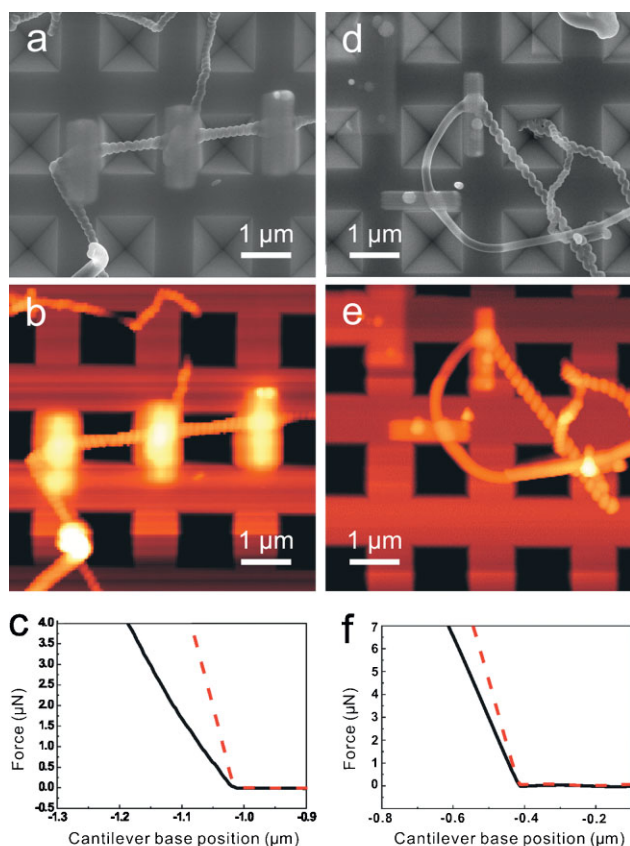


Figure 5. SEM and AFM images, and typical F - D curves of helical and straight nanotubes suspended above the pits of a Si substrate. a) SEM image, b) AFM image, and c) curve of a helical nanotube with an outer diameter of 123 nm. d) SEM image, e) AFM image, and f) curve of a straight nanotube (produced from a nanofiber containing both straight and coiled sections) with an outer diameter of 131 nm. The black solid and red dashed lines in (c) and (f) represent F - D curves measured at the nanotubes suspended across the pits and on the substrates, respectively.

circular cross section. When a beam deflects by ΔZ for a given force f at the midpoint, the bending modulus E_b can be derived from the F - D curve using the equation:^[22,23]

$$E_b = \frac{L^3}{192I} \frac{f}{\Delta Z} \quad (1)$$

where L is the suspended length and I is the second moment of area of the beam, which for a filled cylindrical beam of outer diameter D is $\pi D^4/64$. The second term in Equation (1) is the given force per unit deflection $f/\Delta Z$ measured by the slope of the F - D curve, which is given by

$$\frac{f}{\Delta Z} = \frac{\tan \alpha \tan \beta}{\tan \beta - \tan \alpha} \quad (2)$$

where $\tan \alpha$ and $\tan \beta$ are the slopes of the F - D curves in the linear regime obtained from the nanotubes on the rigid substrate and across the pits. From the above relationship of

Equation (2), Equation (1) can be written as follows:

$$E_b = \frac{L^3}{3\pi D^4} \frac{dF}{d\delta} = \frac{L^3}{3\pi D^4} \frac{\tan \alpha \tan \beta}{\tan \beta - \tan \alpha} \quad (3)$$

Figure 5c and f show typical F - D curves obtained from the nanotubes suspended across the pits (black solid line) and on the rigid substrate (red dashed line). The $\tan \alpha$ and $\tan \beta$ were extracted from the slopes of these F - D curves. To minimize the error for the calculation of the elastic modulus, the suspended length and the outer diameter of the nanotubes were determined from SEM images. The bending elastic modulus E_b was obtained using these slopes, dimensions, and Equation (3). We find that the moduli of the helical and straight nanotubes are 30.1 and 112.0 GPa, respectively. Interestingly, the modulus of the helical nanotube is nearly four times smaller than that of the straight nanotube. This indicates that the helical nanotubes are much more flexible due to their geometry.^[24] In general, the helical nanostructures can have a large degree of deformation, that is, superior elastic properties, due to their small sizes and/or dislocation.^[24,25] For the present helical nanotubes, the small thickness of the nanotubes without introducing dislocation probably leads to a large degree of flexibility and elasticity because of their amorphous structures.^[24]

In conclusion, various helical oxide nanotubes were synthesized by ALD using carbon nanocoils as sacrificial templates followed by thermal annealing in air. Multilayer helical nanotubes were also obtained by sequential ALD of different materials. In addition, ternary helical nanotubes, such as spinel aluminate, could also be prepared by a solid-state reaction between two different ALD coatings. These nanotubes perfectly replicated the helical morphology of the initial templates. ALD shows an absolute advantage over other technologies to coat the high-curvature surfaces of helical nanostructures with conformal and precisely controlled thicknesses. The availability of a large number of precursors for ALD provides us with the capability to synthesize numerous helical oxide nanotubes besides those mentioned above. These helical oxide nanotubes show a much smaller elastic modulus than straight nanotubes. Therefore, they have many potential applications in the fields of nanosensors, mechanical springs, actuators, and elastic electric conductors due to their elastic properties.

Experimental Section

The carbon nanocoils used in this work were synthesized by CVD using acetylene as a carbon source and copper nanoparticles as catalysts at 250 °C as reported previously.^[26] ALD of various oxides was carried out in a hot-wall flow-type ALD reactor (SUNALE R75, Picosun, Finland), except for SiO₂ which was deposited in a chamber-type reactor (Savannah system from Cambridge Nanotech. Inc.). Prior to ALD, the carbon nanocoils were dispersed in ethanol by ultrasonic agitation and then dropped onto a Si wafer. After the samples were dried at ambient temperature, they

were transferred into the ALD chamber. For Al₂O₃, ZnO, TiO₂, and HfO₂ deposition, trimethylaluminum (TMA), diethylzinc (ZnEt₂), titanium tetraisopropyl oxide (TIP), and tetrakis(dimethylamino)-hafnium (TDMAH) were used as metal precursors, respectively. Deionized H₂O was used as an oxygen reactant source. Deposition temperatures for Al₂O₃, TiO₂, and HfO₂ were 150 °C. ZnO deposition was performed at 100 °C. TMA, ZnEt₂, and H₂O were kept at 20 °C. TIP and TDMAH were kept at 60 and 80 °C, respectively. SiO₂ was deposited with 3-aminopropyltriethoxysilane (H₂N(CH₂)₃Si(OCH₂CH₃)₃), H₂O, and O₃ as reported previously.^[27] To remove the carbon cores after ALD and obtain helical nanotubes, the coated samples were annealed in a tube furnace in air at 500 °C for 1 h.

For TEM analysis, the structures were dispersed in ethanol by sonication for 10 s. Several drops of the suspension were dropped onto a carbon-coated TEM Cu grid and dried at ambient temperature. A JEM 1010 microscope operated at 100 kV was used to take images of the structures.

For the mechanical property measurements of helical Al₂O₃ nanotubes, several drops of nanocoil suspension were dispersed on a Si substrate with square-shaped pits (inverted pyramids) with a lateral size of ≈1.2 μm and a depth of ≈700 nm, which was prepared by photolithographic pre patterning and subsequent alkaline etching.^[28] The nanocoil templates were subsequently removed by annealing the sample in air after Al₂O₃ deposition. Nanotubes aligned across pits could be found by SEM. To provide the mechanical rigidity to prevent the nanotubes from slipping during the bending test, Pt pads ≈200 nm in thickness were deposited on both ends of the nanotubes using electron-induced deposition in an FEI dual-beam focused ion beam system (Nova Nanolab 600).^[21] The deposited Pt pads had a rectangular shape. The location of each nanotube was marked for subsequent mechanical measurements. A commercial AFM instrument (Park Systems, XE-100) with its software was used to conduct bending tests on nanotubes in air at room temperature. Si cantilevers with calibrated force constants ranging from 40 to 45 N m⁻¹ were used to perform bending tests.^[29] The x–y and z scanners for the microscope used in the bending tests were calibrated according to the procedures provided by Park Systems. During the F–D measurements, the AFM tip was positioned at the midpoint of each nanotube. For comparison, a reference sample with a straight nanotube was also prepared and measured. The straight (helical) nanotube shown in Figure 5 had a suspended length of 1330 (1200) nm and an outer diameter of 131 (123) nm according to the SEM images. Each elastic modulus was obtained from more than five measurements. The geometry of the nanotubes can be the main factor affecting their elastic modulus because both nanotubes have similar dimensions.

Keywords:

atomic layer deposition · carbon nanocoils · helical structures · nanotubes · templates

- [1] S. Amelinckx, X. B. Zhang, D. Bernaerts, X. F. Zhang, V. Ivanov, J. B. Nagy, *Science* **1994**, *265*, 635.
- [2] S. Motojima, M. Kawaguchi, K. Nozaki, H. Iwanaga, *Appl. Phys. Lett.* **1990**, *56*, 321.
- [3] V. K. Varadan, R. D. Hollinger, V. V. Varadan, P. K. Sharma, *Smart Mater. Struct.* **2000**, *9*, 413.
- [4] M. Zhang, Y. Nakayama, L. Pan, *Jpn. J. Appl. Phys. Part 2* **2000**, *39*, L1242.
- [5] H. F. Zhang, C. M. Wang, E. C. Buck, L. S. Wang, *Nano Lett.* **2003**, *3*, 77.
- [6] J. H. Jung, Y. Ono, K. Hanabusa, S. Shinkai, *J. Am. Chem. Soc.* **2000**, *122*, 5008.
- [7] H. F. Zhang, C. M. Wang, L. S. Wang, *Nano Lett.* **2002**, *2*, 941.
- [8] S. Kobayashi, N. Hamasaki, M. Suzuki, M. Kimura, H. Shirai, K. Hanabusa, *J. Am. Chem. Soc.* **2002**, *124*, 6550.
- [9] J. H. Jung, H. Kobayashi, K. J. C. van Bommel, S. Shinkai, T. Shimizu, *Chem. Mater.* **2002**, *14*, 1445.
- [10] Y. Q. Qu, J. D. Carter, T. Guo, *J. Phys. Chem. B* **2006**, *110*, 8296.
- [11] X. Y. Kong, Z. L. Wang, *Nano Lett.* **2003**, *3*, 1625.
- [12] G. W. Xie, Z. B. Wang, Z. L. Cui, Y. L. Shi, *Carbon* **2005**, *43*, 3181.
- [13] H. Ogihara, M. Sadakane, Y. Nodasaka, W. Ueda, *Chem. Mater.* **2006**, *18*, 4981.
- [14] S. Motojima, T. Suzuki, Y. Noda, A. Hiraga, S. Yang, X. Chen, H. Iwanaga, T. Hashishin, Y. Hishikawa, *J. Mater. Sci.* **1999**, *39*, 2663.
- [15] R. H. A. Ras, M. Kemell, J. De Wit, M. Ritala, G. Ten Brinke, M. Leskelä, O. Ikkala, *Adv. Mater.* **2007**, *19*, 102.
- [16] C. F. Herrmann, F. H. Fabreguette, D. S. Finch, R. Geiss, S. M. George, *Appl. Phys. Lett.* **2005**, *87*, 123110.
- [17] M. Knez, A. Kadri, C. Wege, U. Gösele, H. Jeske, K. Nielsch, *Nano Lett.* **2006**, *6*, 1172.
- [18] Q. Peng, X. Y. Sun, J. C. Spagnola, G. K. Hyde, R. J. Spontak, G. N. Parsons, *Nano Lett.* **2007**, *7*, 719.
- [19] Y. Qin, X. Jiang, Z. L. Cui, *J. Phys. Chem. B* **2005**, *109*, 21749.
- [20] H. J. Fan, M. Knez, R. Scholz, K. Nielsch, E. Pippel, D. Hesse, M. Zacharias, U. Gösele, *Nat. Mater.* **2006**, *5*, 627.
- [21] B. Varghese, Y. Zhnag, L. Dai, V. B. C. Tan, C. T. Lim, C.-H. Sow, *Nano Lett.* **2008**, *8*, 3226.
- [22] Q. Xiong, N. Duarte, S. Tadigadapa, P. C. Eklund, *Nano Lett.* **2006**, *6*, 1904.
- [23] K. Lee, B. Lukic, A. Margrez, J. W. Seo, G. A. D. Briggs, A. J. Kulik, L. Forró, *Nano Lett.* **2007**, *7*, 1598.
- [24] P. X. Gao, W. Mai, Z. L. Wang, *Nano Lett.* **2006**, *6*, 2536.
- [25] H.-F. Zhang, C.-M. Wang, L.-S. Wang, *Nano Lett.* **2002**, *2*, 941.
- [26] Y. Qin, Z. K. Zhang, Z. L. Cui, *Carbon* **2003**, *41*, 3072.
- [27] J. Bachmann, R. Zierold, Y. T. Chong, R. Hauert, C. Sturm, R. Schmidt-Grund, B. Rheinländer, M. Grundmann, U. Gösele, K. Nielsch, *Angew. Chem.* **2008**, *120*, 6272; *Angew. Chem. Int. Ed.* **2008**, *47*, 6177.
- [28] V. Lehmann, *J. Electrochem. Soc.* **1993**, *140*, 2836.
- [29] J. L. Hutter, J. Bechhoefer, *Rev. Sci. Instrum.* **1993**, *64*, 1868.

Received: November 16, 2009

Revised: February 11, 2010